

# **Hair follicle stem cell cultures reveal self-organizing plasticity of stem cells and progeny**

Carlos Andrés Chacón-Martínez, Markus Klose, Catherin Niemann, Ingmar Glauche,  
Sara A. Wickström

## **Table of contents Appendix**

### **Appendix supplementary materials and methods**

#### **Appendix figures**

Appendix figure S1. Establishment of a HFSC culture system

Appendix figure S2. Cells from 3C cultures give rise to holoclones in colony forming assays and maintain their multipotency upon to freeze-thaw cycles

Appendix figure S3. Comparison of *in vivo* CD34<sup>+</sup>α6<sup>+</sup> HFSC and 3C transcriptomes

Appendix figure S4. 3C cultures evolve into a stable population equilibrium of HFSCs and non-HFSCs

Appendix figure S5. Dynamic interconversion of non-HFSCs and HFSCs in 3C cultures

Appendix figure S6. Shh and BMP signaling control HFSC fate in 3C cultures

## Appendix supplementary materials and methods

### Mathematical model

In order to describe the temporal behavior of HFSC and non-HFSC numbers in 3C cultures, we designed a four-compartment model (two compartments per cell type for proliferating cells and pre-apoptotic cells, respectively, see Figure 4C). We describe the cell numbers within these compartments and the transitions between them by ordinary differential equations (ODEs) as follows:

$$\begin{aligned}\dot{N}_{SC}(t) &= p_{SC,max} \left( 1 - \frac{N_{SC}(t) + N_P(t) + N_{AP_{SC}}(t) + N_{AP_P}(t)}{K} \right) N_{SC}(t) \\ &\quad + t_{P \rightarrow SC} N_P(t) - t_{SC \rightarrow P} N_{SC}(t) - ap_{SC} N_{SC}(t) \\ \dot{N}_P(t) &= p_{P,max} \left( 1 - \frac{N_{SC}(t) + N_P(t) + N_{AP_{SC}}(t) + N_{AP_P}(t)}{K} \right) N_P(t) \\ &\quad + t_{SC \rightarrow P} N_{SC}(t) - t_{P \rightarrow SC} N_P(t) - ap_P N_P(t) \\ \dot{N}_{AP_{SC}}(t) &= ap_{SC} N_{SC}(t) - deg \cdot N_{AP_{SC}}(t) \\ \dot{N}_{AP_P}(t) &= ap_P N_P(t) - deg \cdot N_{AP_P}(t)\end{aligned}$$

Herein, all rates are given in units of cells per hour. Terms with interconversion rates  $t_{SC \rightarrow P}$  and  $t_{P \rightarrow SC}$  refer to the conversion between HFSCs ( $N_{SC}$ ) and non-HFSCs ( $N_P$ ). Transition into a pre-apoptotic state is described by the terms with the apoptosis rates  $ap_{SC}$  and  $ap_P$ . Pre-apoptotic cells ( $N_{AP_{SC}}$  and  $N_{AP_P}$ , respectively) are assumed to be degraded with rate  $deg = 1/12$  [cells/hour]. These rates are independent from the cell numbers in the culture. Cell proliferation is described by a logistic growth dynamic as suggested by Appendix figure S4B, in which an initial growth phase within the first six days is followed by a stable equilibrium with an approximately constant absolute cell number (resulting from the growth limitation at the carrying capacity  $K$ ). The rates  $p_{SC,max}$  and  $p_{P,max}$  refer to the maximum proliferation rates (i.e. for an empty system), while  $p_{SC,eff}(t) = p_{SC,max} \left( 1 - \frac{N_{SC}(t)}{K} \right)$  and  $p_{P,eff}(t) = p_{P,max} \left( 1 - \frac{N_P(t)}{K} \right)$  correspond to the “effective proliferation rates” at time  $t$  which depend on the absolute cell number present within the culture.

We were interested in estimating the interconversion rates  $t_{SC \rightarrow P}$  and  $t_{P \rightarrow SC}$  which describe the transition between HFSC and non-HFSC state. Therefore, we aimed to find a choice of rate parameters that would optimally describe the measured data. Technically, this was achieved by identifying the parameter values that maximize the likelihood of observing the experimentally obtained data given the parameters (maximum likelihood estimation, MLE).

First, we used time course data for (Ia) primary cell cultures (Figure 4A) and (Ib) purified cell cultures (Appendix figure S4B) to estimate the model parameters. Second, we applied the same procedure to derive model parameters for the time course data of FACS-purified (IIa)  $CD34^+ \alpha 6^+$  cells (HFSCs, Figures 5B and Appendix figure S5D, grey lines) and (IIb)  $CD34^- \alpha 6^+$  cells (non-HFSCs, Figures 5C and Appendix figure S5E, grey lines). In both respective fitting procedures, we solved our ODE system separately for the respective scenarios (a) and (b) with the same set of parameters. Simulated data was then evaluated at the relevant time points for which experimental measures were available. For comparison with the absolute cell numbers, we computed the residual sum of squares on a normalized scale obtained by dividing the absolute cell numbers by their maximum value.

In order to reduce the number of free rate parameters, we incorporated some prior knowledge into the optimization routine:

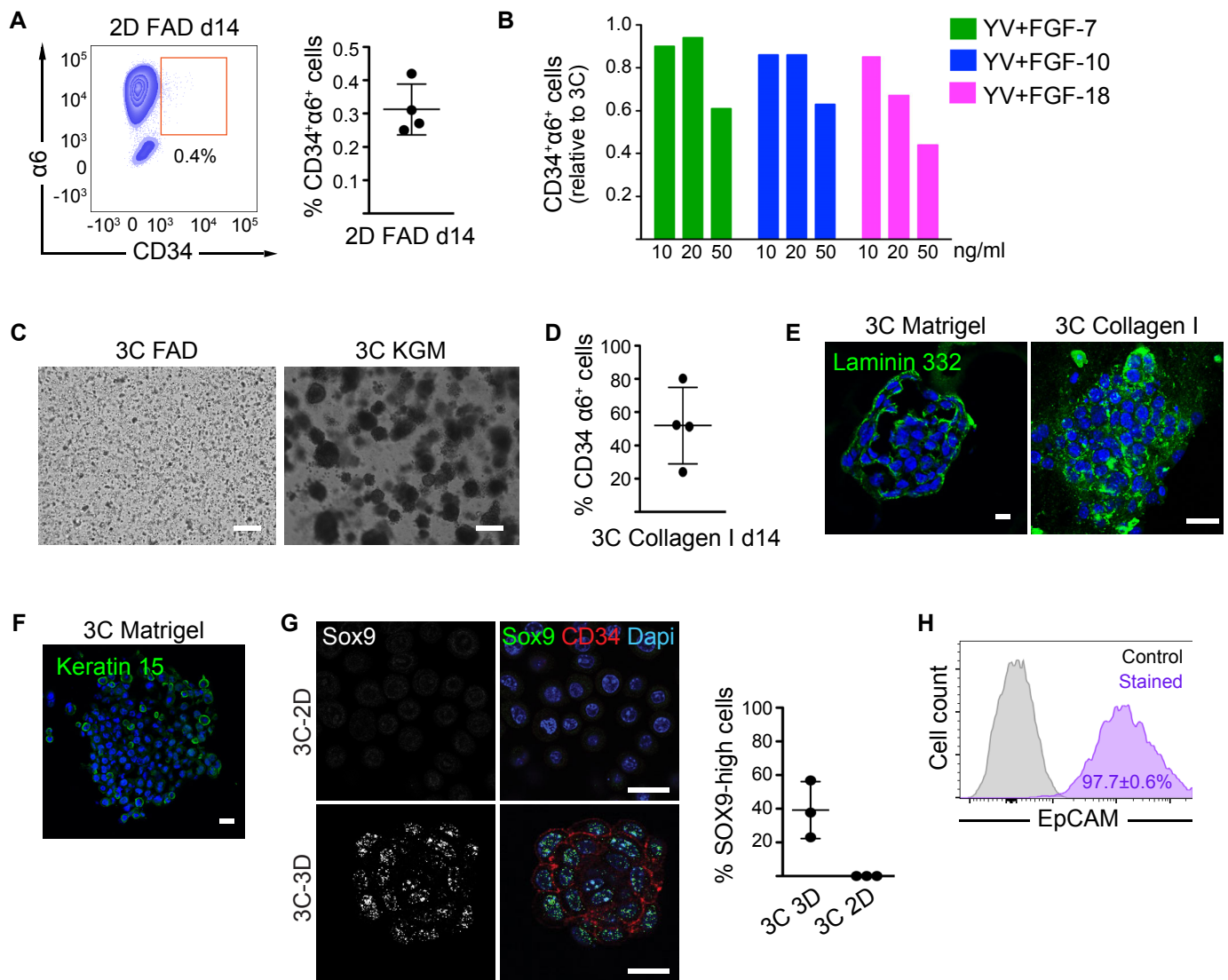
- Apoptosis rates were estimated by using Annexin V+ staining data belonging to (I) Appendix figure S4B and (II) Appendix figures S5D+E. We assumed that cells first enter a pre-apoptotic state (similar to becoming Annexin V+) described by entrance into the pre-apoptotic compartments  $N_{AP_{SC}}$  and  $N_{AP_P}$ , respectively, where they are on average degraded after 12 hours (which corresponds to a degradation rate of  $deg = 1/12$  cells per hour). Annexin V+ data suggest that the rates of both HFSCs and non-HFSCs to become pre-apoptotic remain rather constant over time and similar for both cell types.
- Independently of the starting values for the optimization routines, the carrying capacity was robustly estimated in the order of (I) 120,000 cells for primary

cell cultures and (II) 220,000 for purified cell cultures. Therefore, we kept this value fixed for all further estimations.

- We used data from the EdU uptake experiments in Figure 4B to estimate division rates of HFSCs and non-HFSCs. We found that HFSCs proliferated faster than non-HFSCs and used a fixed ratio of (I)  $\frac{p_{SC,EdU}}{p_{P,EdU}} \approx 1.65$  and (II)  $\frac{p_{SC,EdU}}{p_{P,EdU}} \approx 1.3$  to account for this increased turnover of HFSCs. Overall, our findings are rather insensitive against moderate variations of these ratios.
- We then estimated the proliferation and interconversion rates of HFSCs to non-HFSCs and vice versa (for the settings (I) and (II), respectively) by using a MLE for both experimental settings (Ia + b) and (IIa + b).

In order to estimate the model parameters for primary cell cultures (I), we used the following data points: Figure 4A, right panel, days 6 to 14, and Appendix figure S4B, left panel, days 14 to 26. The ODE system was initialized with the cell numbers measured at day 6 (Ia) and day 14 (Ib), respectively. MLE results are shown in Figures 4D and Appendix figure S4D.

In order to estimate the model parameters for FACS-purified cell cultures (II), we used the following data points: Figures 5B+C, days 2 to 10, and Appendix figures S5D+E (grey lines), days 2 to 10. Day 0 was left out due to the initial drop in cell numbers (see Appendix figures S5D+E), which cannot be explained by our simple mathematical model. Consequently, the initial cell numbers at day 0 were estimated by the MLE procedure together with the proliferation and interconversion rates by assuming that the initial cell number ratios of HFSCs to non-HFSCs are given by 99:1 (IIa) and 1:99 (IIb). The estimated initial cell numbers ( $N_{SC}(0) = 1455$ ,  $N_P(0) = 15$  for (IIa) and  $N_{SC}(0) = 4$ ,  $N_P(0) = 413$  for (IIb)) provide an approximation of the number of cells contributing to the observed population dynamics in the long run. MLE results are shown in Figures 5D+E and Appendix figure S5D+E.



### Appendix figure S1 (Related to Figure 1) Establishment of a HFSC culture system

**A.** Cells were grown in 2D in FAD medium on mitomycin-treated feeder cells for 14 days. CD34<sup>+</sup>α6<sup>+</sup> cells were quantified by flow cytometry. Representative FACS plot and quantification (n=4; mean ±SD) are shown.

**B.** Several FGF isoforms in combination with VEGF and Y27632 can support expansion of CD34<sup>+</sup>α6<sup>+</sup> cells in 3D matrigel cultures. Cells were grown in the indicated medium for 14 days before quantification of CD34<sup>+</sup>α6<sup>+</sup> cells by flow cytometry. Data were normalized to cells grown in 3C conditions (3D-Matrigel in KGM + Y27632 + VEGF + FGF-2). YV: Y27632 + VEGF

**C.** Phase contrast images of cells grown in 3C FAD (3D-Matrigel in FAD + Y27632 + VEGF + FGF-2) or in 3C KGM (3D-Matrigel in KGM + Y27632 + VEGF + FGF-2). Note that cells fail to survive in 3C FAD. Scale bars 250 μm.

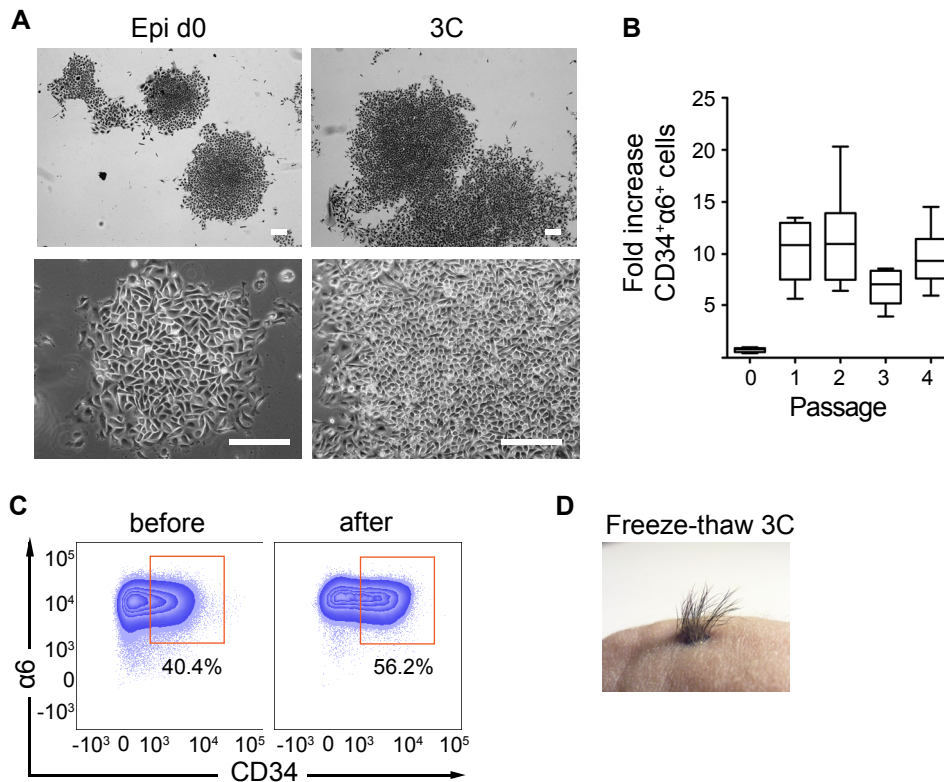
**D.** Cells were grown 3D Collagen I gels in 3C medium for 14 days. CD34<sup>+</sup>α6<sup>+</sup> cells were quantified by flow cytometry (n=4; mean ±SD).

**E.** Immunofluorescence analysis of 3C cultures in Matrigel or Collagen I shows that the cells express and deposit Laminin 332. Scale bars 25 μm.

**F.** Immunofluorescence analysis of 3C cultures in Matrigel shows that the cells express and express the HFSC marker Keratin-15 (F). Scale bars 25 μm.

**G.** Immunofluorescence analysis and quantification (n=3; mean ±SD) of cells grown in 3C cultures (3C-3D) or in 2D in 3C medium (3C-2D) show SOX9 expression only in 3C-3D. Scale bar 25 μm

**H.** EpCAM expression in 3C cultures quantified by flow cytometry. A representative histogram and quantification (n=6; mean ±SD) are shown.



### Appendix figure S2 (Related to Figure 2)

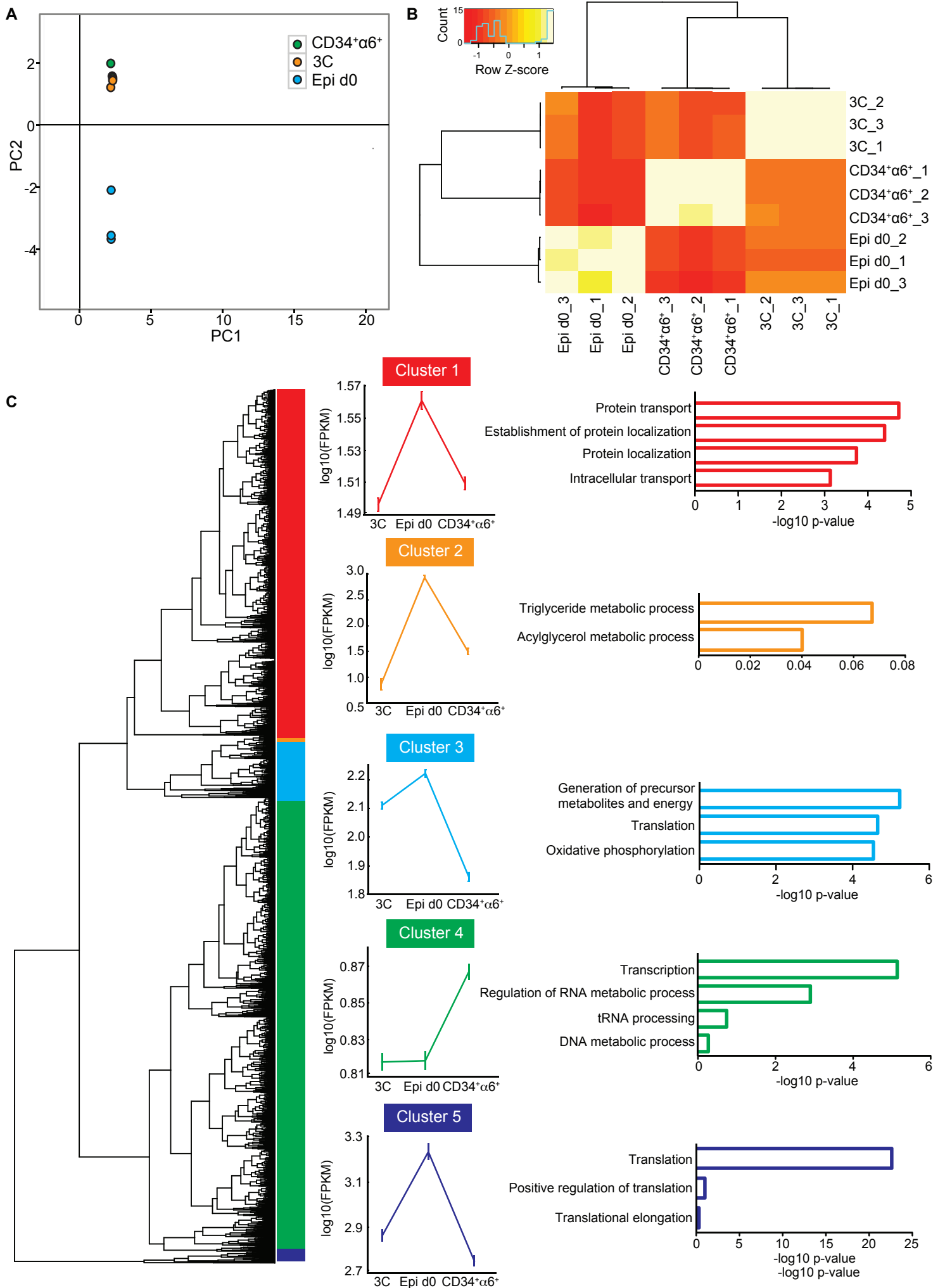
#### Cells from 3C cultures give rise to holoclones in colony forming assays and maintain their multipotency upon freeze-thaw cycles

**A.** Representative images of colonies generated by the indicated cells in colony forming assays. Low (upper panels) and high (lower panels) magnification images of colonies. Scale bar 100  $\mu$ m. Epi d0: freshly isolated epidermal cells; 3C: cells grown 14 days in 3D-Matrigel in KGM + Y27632 + VEGF + FGF-2.

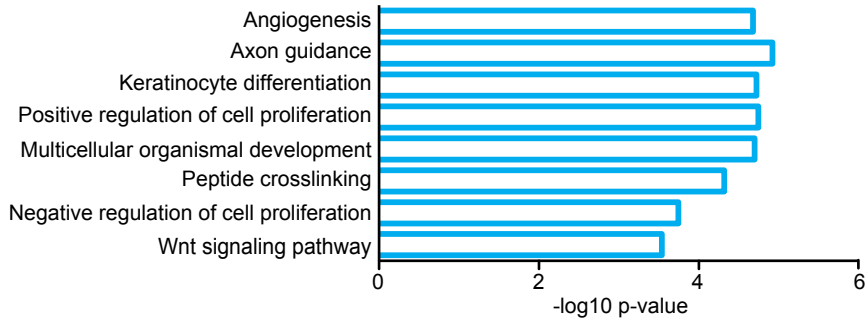
**B.** 3C cultures maintain long-term proliferative potential of CD34<sup>+</sup>α6<sup>+</sup> cells. Passaging of cells in 3C was performed as in Figure 2C. Data are shown using a Box-and-Whisker plot: box indicates 25th and 75th percentiles; error bars represent 10th and 90th percentiles; middle line is the median, n=6 independent experiments.

**C.** 3C-cultured cells withstand freeze-thaw cycles. Passage 1 cells in 3C cultures (labeled: before) were frozen for 3 months in liquid nitrogen, thawed and subsequently cultured for additional 14 days (labeled: after) prior to FACS analysis.

**D.** 3C-cultured cells maintain multipotency upon freeze-thaw cycles. Full thickness skin reconstitution assay with passage 1 3C-cultured cells that were frozen for 3 months in liquid nitrogen, thawed and subsequently cultured for additional 14 days prior to transplantation. A representative recipient of 3 mice is shown.



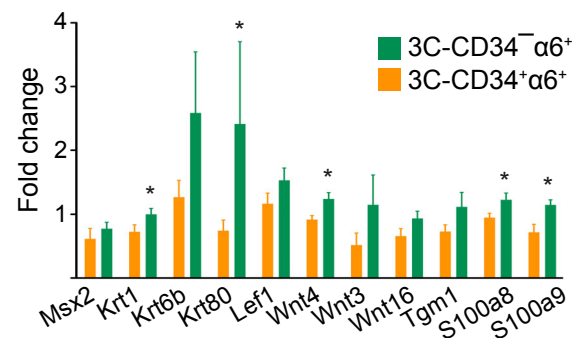
Appendix figure S3 (Related to Figure 3)

**D****E**

	Gene set	ES	NES	FDR q-val	Top ranked gene set members
ENRICHED in CD34 <sup>+</sup> α6 <sup>+</sup>	1. Naba Core Matrisome	-0.60	-2.63	0.0000	Igfbp5, Col6a1, Col6a2, Hmcn1, Ltbp2, Npnt, Dcn
	2. Reactome NCAM1 interactions	-0.79	-2.31	0.0000	Col6a1, Col6a2, Col8a2, Col5a1, Col5a2, Col4a2, Col1a1
	3. Reactome NCAM1 signaling	-0.71	-2.29	0.0000	Col6a1, Col6a2, Gfra1, Sptb, Col1a1, Col5a2, Cacnb1
ENRICHED in 3C	1. Zhang response to Ikk inhibitor and Tnf up	0.61	3.06	0.0000	Krt6b, Cxcl2, Sprr1a, Inhba, Tnfaip2, Il1a
	2. Rickman tumor differentiated well vs moderately dn	0.65	2.90	0.0000	Sprr1b, Krt6b, Krt16, Prr9, Nrg1, Cpa4
	2. Rickman tumor differentiated well vs poorly dn	0.54	2.88	0.0000	Sprr1b, Krt6b, Krt16, Prr9, Inhba, Nrg1,

**F**

	UP in CD34 <sup>+</sup> α6 <sup>+</sup>	UP in 3C
Cell cycle	Cdk14, Cdkn2c, Cdkn1b, Cdkn2d	Ccng1, Ccnd1, Ccne1, Cdkn2a, Cdkn2b
Extracellular matrix organization	Tnxb, Hspg2, Postn, Ctgf, Col4a6, Col6a1, Col6a2, Col8a2, Col5a1, Col5a2, Col4a2, Col1a1	Fbln2, Nid1
Wnt signaling	Dkk3, Sfrp1, Fzd3, Fzd5, Wnt16, Wnt3, Wnt5b	Wnt3a, Wnt4, Wnt5a, Wnt7a, Wnt10a, Wnt10b, Porcn
Keratinocyte differentiation	Krt10, Cd109, Ptch1	Foxn1, Tgm1, Sprra1, Sprr2a, Lca1a1, Lce1h, Lce1f, Lce1i

**G****Appendix figure S3 (Related to Figure 3)****Comparison of in vivo CD34<sup>+</sup>α6<sup>+</sup> HFSC and 3C transcriptomes**

**A-B.** Principal component analysis (A) and Pearson's correlation distance (B) of RNA sequencing data from three biological replicates of freshly isolated epidermal cells (Epi d0), 3C-cultured cells (3C) and FACS-purified CD34<sup>+</sup>α6<sup>+</sup> HFSCs (CD34<sup>+</sup>α6<sup>+</sup>) show that transcriptomes of 3C cells more closely resemble CD34<sup>+</sup>α6<sup>+</sup> HFSCs than Epi d0 cells.

**C.** Dendrogram of gene-to-gene euclidian distance correlation and subsequent distance-based gene clustering identifies 5 clusters of genes with similar expression levels in 2 of the 3 groups. Note that 3 clusters show similar transcript levels in CD34<sup>+</sup>α6<sup>+</sup> and 3C cells. GO term analysis of the different clusters are shown.

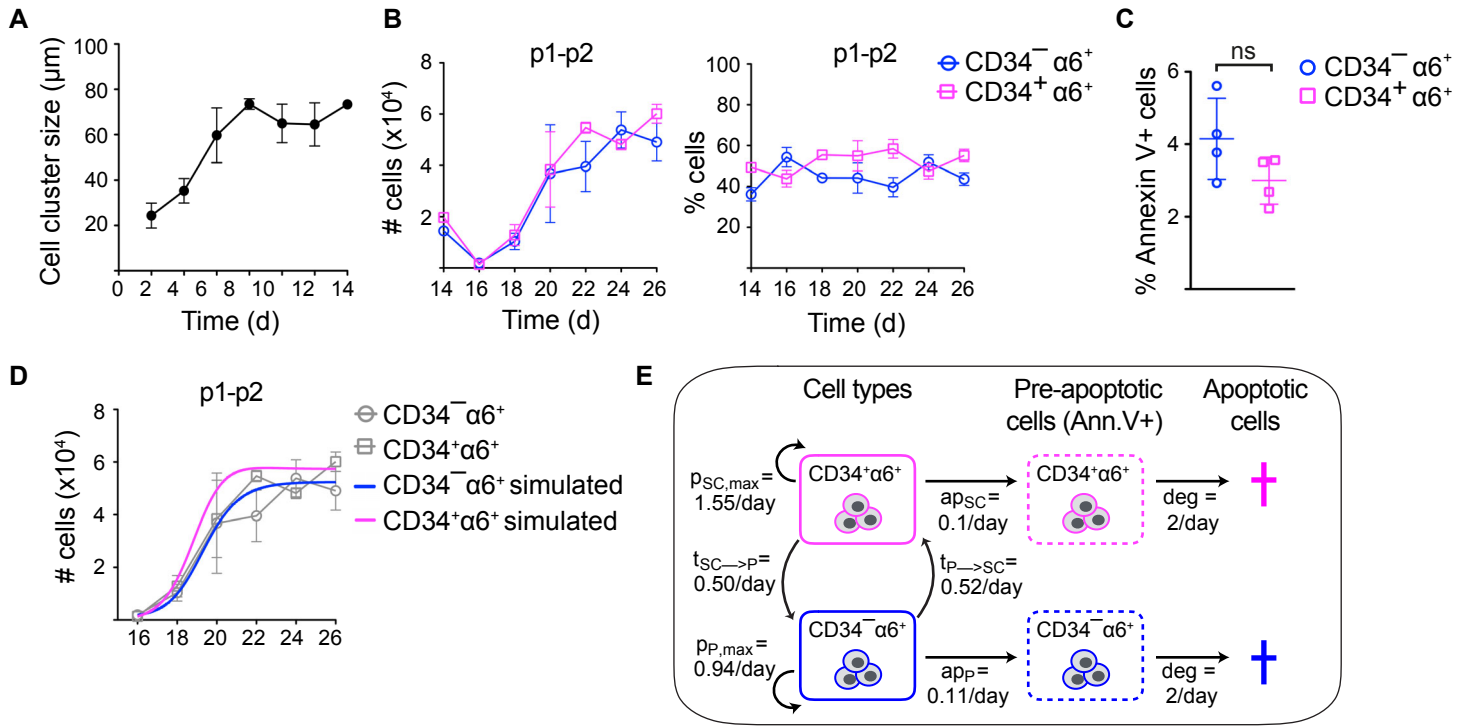
**D.** GO term analysis of the differentially expressed genes between CD34<sup>+</sup>α6<sup>+</sup> and 3C.

**E.** GSEA analysis of most significantly overrepresented pathways in differentially expressed genes between CD34<sup>+</sup>α6<sup>+</sup> and 3C.

**F.** Selected most significantly differentially expressed genes representing biological processes identified in GO term and GSEA analyses.

**G.** RT-qPCR analysis confirms upregulation of genes reported to be enriched in HFSC progeny in 3C-CD34<sup>-</sup>α6<sup>+</sup> cells (mean ±SEM; n=4; \*p ≤ 0.05, Mann-Whitney U test).





#### Appendix figure S4 (Related to Figure 4)

#### 3C cultures evolve into a stable population equilibrium of HFSCs and non-HFSCs

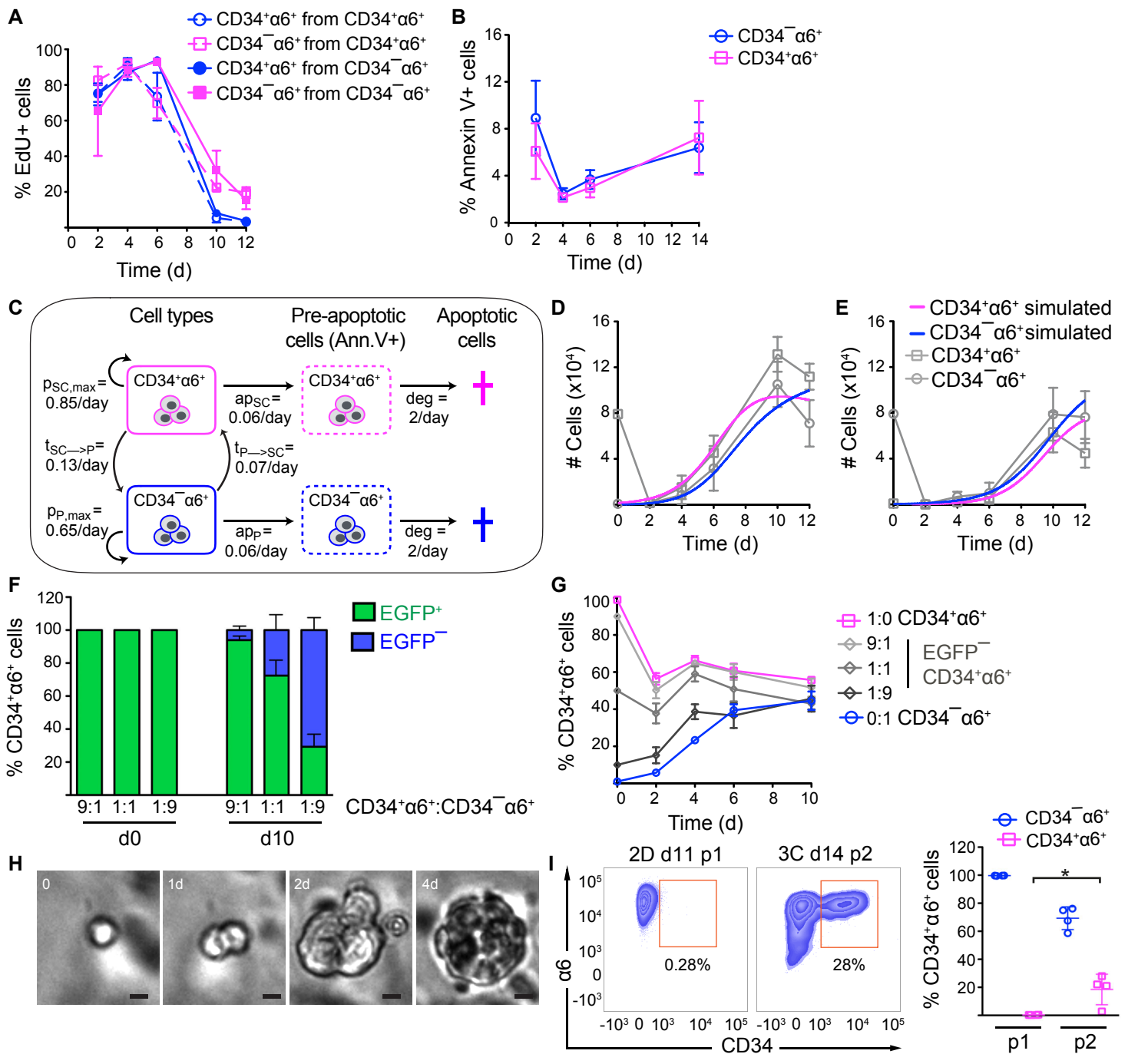
**A.** Quantification of cell cluster size in 3C cultures over time ( $n=4$  independent experiments; mean  $\pm$  SEM).

**B.** FACS analysis of CD34 $^+$  $\alpha$ 6 $^+$  cells between day 14 and 26 of culture (p1-p2) shows that 3C cultures maintain a stable population equilibrium over long periods. Cells were first cultured for 14 days, then passaged and cultured for another 12 days (p1-p2;  $n=4$ ; mean  $\pm$  SEM).

**C.** Cells from day 10 3C cultures were stained with Annexin V antibodies to detect apoptotic cells followed by quantification using flow cytometry ( $n=4$ ; mean  $\pm$  SD; ns: not significant, Mann-Whitney U-test).

**D.** Simulated growth rates for days 16-26 (p1-p2) from the steady state mathematical model (colored lines) estimated from the data in panel B (grey lines).

**E.** Schematic illustration of the steady state mathematical model with estimated interconversion rates. HFSCs (CD34 $^+$  $\alpha$ 6 $^+$ ) and non-HFSCs (CD34 $^-$  $\alpha$ 6 $^+$ ) have a maximum proliferation rate of  $p_{SC,max}$  and  $p_{P,max}$ , respectively. Cells enter apoptosis with rates  $ap_{SC}$  and  $ap_P$  and are both degraded with a rate  $deg$ . Non-HFSCs can convert to HFSCs with a rate  $t_{P \rightarrow SC}$  and vice versa with a rate  $t_{SC \rightarrow P}$ . For clarity rates are given in units of cells/day.



### Appendix figure S5 (Related to Figure 5)

#### Dynamic interconversion of non-HFSCs and HFSC in 3C cultures

**A.** Proliferation in 3C cultures established from FACS-purified  $CD34^+\alpha6^+$  or  $CD34^-\alpha6^+$  cells from p0 3C cultures. Cells were EdU-labeled for 24 h prior to analysis by flow cytometry ( $n=4$ ; mean  $\pm$ SD).

**B.** Apoptosis in 3C cultures as in A. Cells were stained with antibodies and Annexin V (apoptotic cells) followed by flow cytometry quantification ( $n=8$ ; mean  $\pm$ SD).

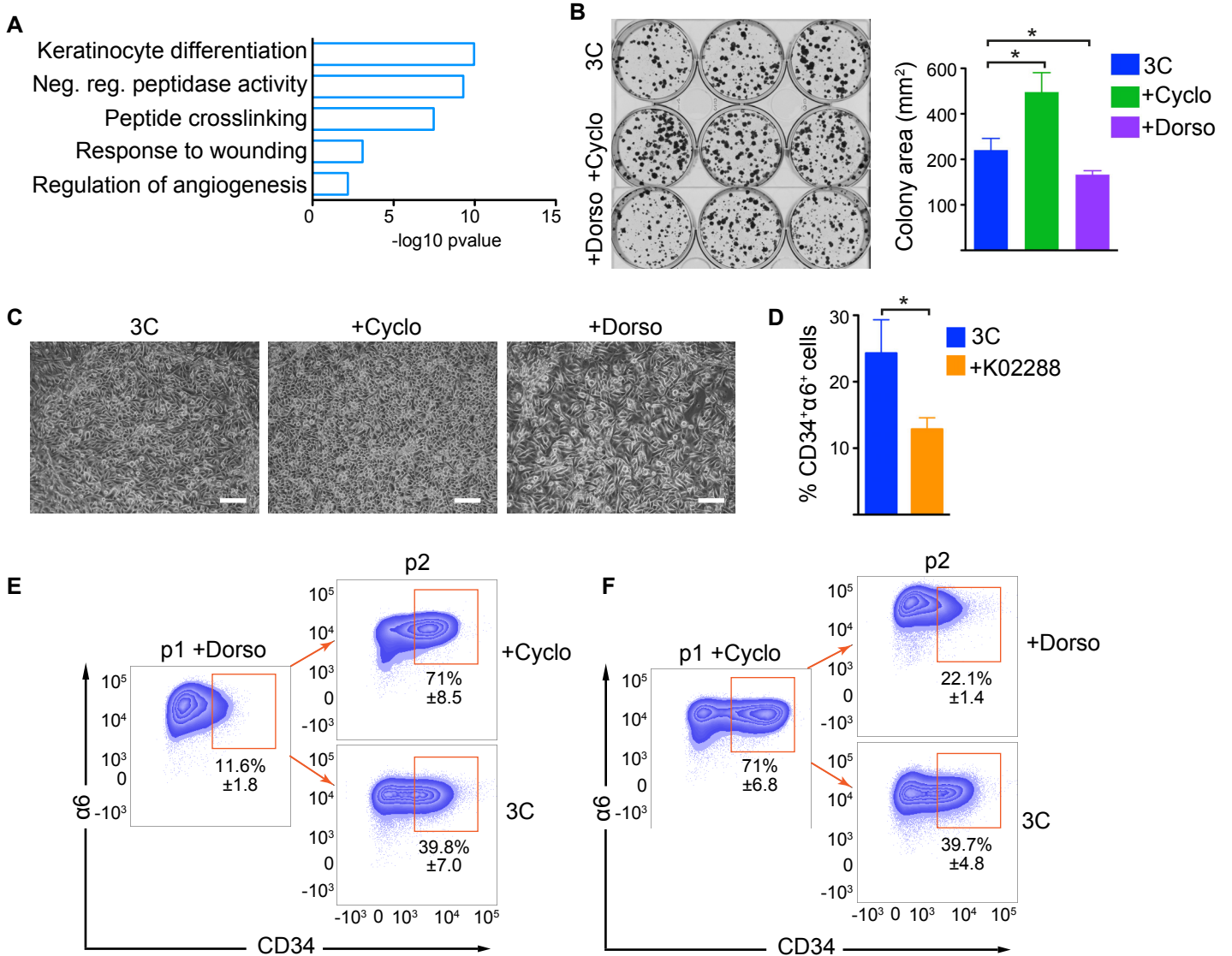
**C.** Schematic illustration of the mathematical model for cultures from purified cells with estimated rates. HFSCs ( $CD34^+\alpha6^+$ ) and non-HFSCs ( $CD34^-\alpha6^+$ ) have a maximum proliferation rate of  $p_{SC,max}$  and  $p_{P,max}$ , respectively. They enter apoptosis with rates  $ap_{SC}$  and  $ap_P$  and are both degraded with a rate  $deg$ . Non-HFSCs can convert to HFSCs with a rate  $t_{P \rightarrow SC}$  and vice versa with a rate  $t_{SC \rightarrow P}$ . For clarity rates are given in units of cells/day.

**D-E.** Simulated growth rates of cultures established with FACS-purified  $CD34^+\alpha6^+$  (D) or  $CD34^-\alpha6^+$  cells (E). Simulations were derived from the mathematical model (colored lines) estimated from the cell frequency data in Figure 5 B-C and absolute cell number data shown as grey lines.

**F-G.** Lineage tracing of FACS-purified  $CD34^+\alpha6^+$  EGFP+ and  $CD34^-\alpha6^+$  EGFP- from p0 3C cultures.  $CD34^+\alpha6^+$  and  $CD34^-\alpha6^+$  were mixed in the indicated ratios on d0 and EGFP expression was used to trace the cells of origin over time by flow cytometry. Proportions of EGFP+ and EGFP-  $CD34^+\alpha6^+$  cells were quantified over time ( $n=4$ ; mean  $\pm$ SD). Presence of EGFP-  $CD34^+\alpha6^+$  cells indicates interconversion (F). 3C cultures reached equilibrium between day 6 and 10 irrespective of the initial proportions of  $CD34^+\alpha6^+$  and  $CD34^-\alpha6^+$  cells (G).

**H.** Snapshots from live cell imaging show formation of a 3C cell cluster from a single cell (scale bars 15  $\mu$ m).

**I.** De novo generation of HFSCs from epidermal cells depleted of HFSCs. Total epidermal cells were cultured in 2D in FAD medium on mitomycin-treated feeder cells for 11 days (2D d11 p1), passaged into 3C and cultured for 14 days (3C d14 p2).  $CD34^+\alpha6^+$  cells were quantified by flow cytometry. Representative FACS plots and quantification are shown ( $n=4$ ; mean  $\pm$ SD; \*  $p \leq 0.05$ , Mann-Whitney U-test).



### Appendix figure S6 (Related to Figure 6)

#### Shh and BMP signaling control HFSC fate in 3C cultures

**A.** GO term analysis of significantly differentially expressed genes from RNAseq experiments from 3C cultures treated for 48 h with Dorsomorphin or Cycloamine.

**B.** Representative images of colonies and quantification of colony forming assays shows that cycloamine treatment increases the colony-forming ability of 3C-cultured cells ( $n=3$ ; mean  $\pm$ SEM; \*  $p \leq 0.05$ , nested ANOVA). 3C: control; +Cyclo: cycloamine; +Dorso: dorsomorphin.

**C.** Representative images of colonies generated by cells in colony forming assays. Note that colonies arising from cycloamine-treated 3C cultures are smaller and more compact than untreated cells, whereas dorsomorphin-treated 3C cultures generate loosely packed colonies with larger cells. Scale bar 100  $\mu$ m.

**D.** Inhibition of BMP signaling with K02288 decreases the numbers of HFSCs. Cells were grown in 3C cultures with the BMP inhibitor K02288 (10 nM) and then analyzed by flow cytometry ( $n=4$ ; mean  $\pm$ SD; \*  $p \leq 0.05$ , Mann-Whitney U-test).

**E, F.** Cultured cells in 3C maintain full plasticity after 4 weeks of culture. Representative FACS plots and quantification are shown ( $n=4$ ; mean  $\pm$ SD). Cells were grown 14 days (p1) in the presence of the indicated inhibitors, then passaged and cultured with or without inhibitors (3C, control) for 14 days.